

IMECE2011-64472

MECHANICAL CHARACTERIZATION AND MODELING OF CORRUGATED METAL FOAMS FOR SOFC APPLICATIONS

Ryan B. Berke
The Ohio State University
Columbus, Ohio, USA
berke.13@osu.edu

Mark E. Walter
The Ohio State University
Columbus, Ohio, USA
walter.80@osu.edu

ABSTRACT

Planar solid oxide fuel cells (SOFCs) are made up of repeating sequences of thin layers of cermet electrodes, ceramic electrolytes, seals, and current-collectors. For electro-chemical reasons it is best to keep the electrolyte layers as thin as possible. However, for electrolyte-supported cells, the thin electrolytes are more susceptible to damage during production, assembly, and operation. The latest-generation electrolyte-supported SOFCs feature metallic foam current-collectors which relay current between the energy-producing materials and the rest of the circuit. These foams are stamped into a corrugated shape which is intended to reduce the compressive loads which are transferred through the stack onto the brittle electrolyte, but the mechanical behavior of the foams remain to be fully understood.

Characterization of the corrugated metal foams consists of comparison of load-vs.-displacement behavior between experimentally measured compression data and a single-component finite element model which isolates the foam from the rest of the stack. Mechanical properties of the foam are found using an iterative approach, in which the material properties used as inputs to the model are changed until the load-displacement data best agrees with experiments. The model explores the influence of elastic and plastic properties in combination with and without friction. Thus obtained, the properties can then be used in a stack model to determine which parameters can best reduce the demands on the electrolyte without sacrificing electrochemical performance.

INTRODUCTION

Planar solid oxide fuel cells (SOFCs) are made up of repeating layers of cermet electrodes, ceramic electrolytes,

seals, interconnects, and current collectors [1]. SOFCs are often characterized in terms of which layer provides the bulk of the mechanical support, typically either the anode or the electrolyte [2]. An advantage of electrolyte support over anode support is that electrolyte-supported cells are less susceptible to failure due to anode reoxidation of cathode reduction. Another advantage is that the porous anodes are generally harder to seal against cross-contamination of fuel and oxidant.

For electro-chemical reasons, it is best to keep the electrolyte as thin as possible. Thinner electrolytes can allow for lower operating temperatures and have lower resistive losses [3], [4]. It is also desirable to produce cells which are wide in area, allowing them to achieve higher power densities. Electrolytes which are wide and thin are at increased risk of being damaged by mechanical loads during manufacture, assembly, and operation.

In order to produce cells which are mechanically robust while electro-chemically efficient, NexTech Materials Ltd. has developed a new planar, electrolyte-supported SOFC which it calls the FlexCell [5]. The hallmark of the FlexCell design is an electrolyte which contains thinner "active" regions supported by a hexagonal mesh, the mechanical performance of which has already been studied [6]. The design also incorporates a pair of corrugated, metal foams which collect electrical current and help form complete circuits by bridging gaps in between the electrodes and the steel interconnects. As the stack undergoes compression, the distribution of loads placed on the fragile electrolyte is largely determined by the shape and mechanical behavior of the neighboring foams.

FIG 1 shows a schematic of the placement of the corrugated foams in context of a full SOFC stack. Each cell contains an electrolyte with a porous anode and cathode bonded

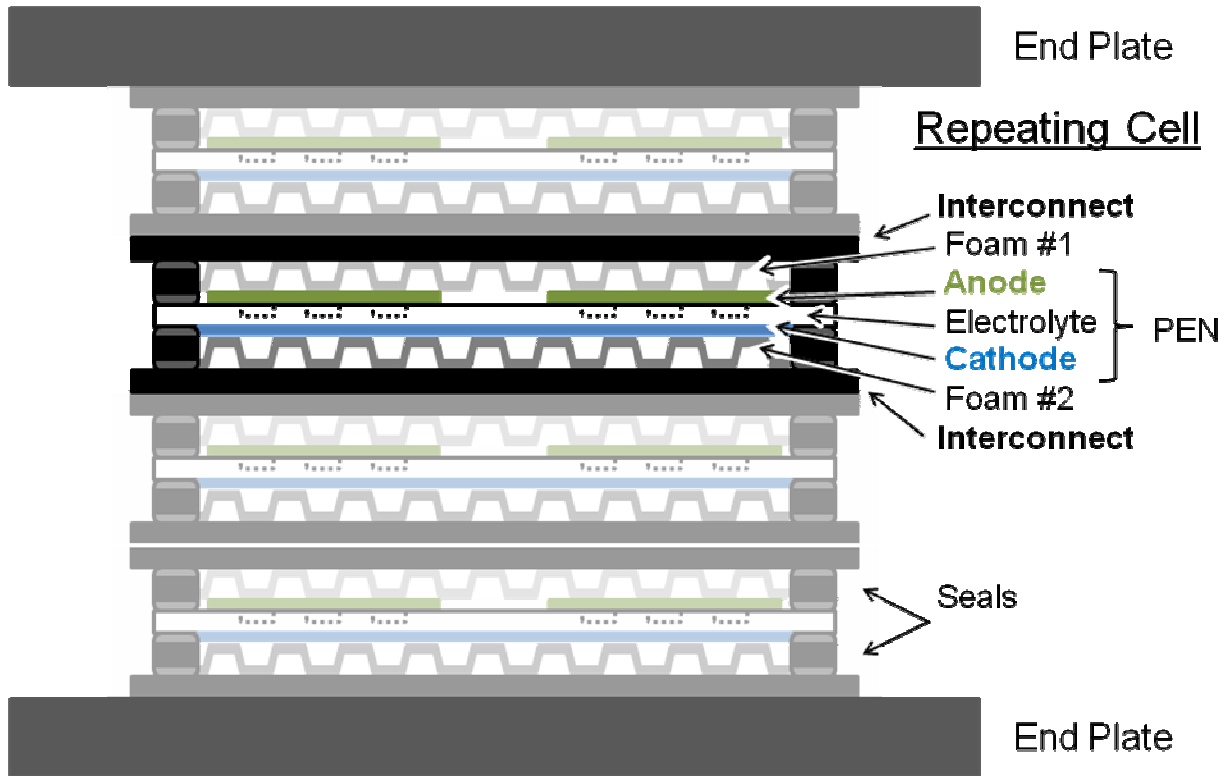


FIG 1: SCHEMATIC OF A PLANAR SOFC ASSEMBLY

to either side, forming an energy-producing assembly that is often referred to as positive electrode - electrolyte - negative electrode, or PEN for short [7]. The cells are bounded by steel interconnects which serve to direct currents, and form a gas-tight separation between adjacent cells. In addition to the two foams, the cells also contain assemblies of seals which further contain and direct gas flows.

The foam on the anode side is a nickel foam, the mechanical properties of which are available in existing literature [8]. The foam on the cathode side is not a true foam, and is Crofer which has been formed into flat sheets of expanded metal mesh, the mechanical behavior of which is unknown. Both metals are then stamped into the corrugated pattern which is used in the FlexCell, as shown in FIG 2.

To ensure robust, efficient designs, the ability to model the

cells using finite element analysis is desirable. Previous work employed a two-scale modeling approach to characterize the mechanical behavior of the electrolyte in absence of the surrounding stack [6]. To study the performance of the electrolyte within the context of a stack, further modeling and experiments must be conducted to characterize the remaining stack components. The focus of this paper is to characterize the cathode-side foam, in particular.

CHARACTERIZATION OF CATHODE-SIDE FOAM

Each foam begins as a flat sheet about 0.15 mm thick, which is then pressed to create corrugations which are evenly distributed. Each corrugation is about 7.2 mm wide, and includes an angle of about 100 degrees between the horizontal and inclined portions of foam. The cathode-side foam uses

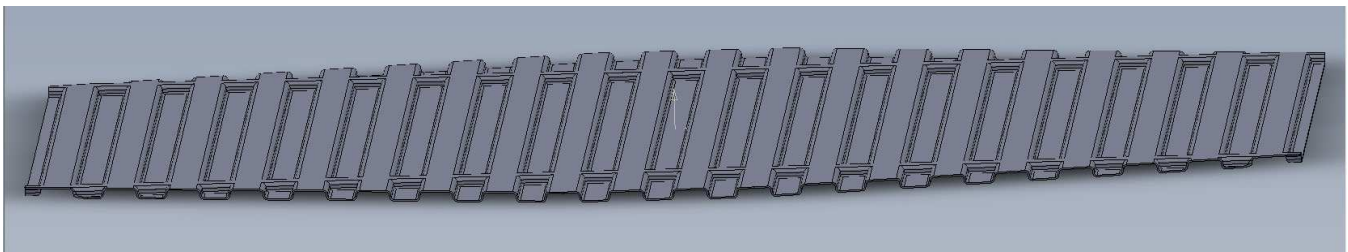


FIG 2: 3-D GEOMETRY FOR THE CURRENT-COLLECTING FOAMS

corrugations which are about 1.5 mm tall. The corrugations in the anode-side foam are about 1.0 mm tall.

The mechanical properties of the foam were determined by comparing experimental compression data against a single-component finite element model which isolates the foam from the rest of the SOFC stack. Since the material properties of the foam are initially unknown, the model was repeated over several iterations using different properties until the load-versus-displacement behavior of the model best agreed with the measurements.

Samples of corrugated foam were compressed between two cylindrical rods in a calibrated load frame. The foams began at an initial height of 1.5 mm and were compressed to a final thickness of 0.1 mm, resulting in the load-displacement data in FIG 3. The rods were about 31.75 mm in diameter. A total of 7 samples were tested, though not all were subjected to the entire range of displacement. The experiments were performed at room temperature, although there are plans to repeat the measurements at temperatures of up to 850 °C.

The load-displacement behavior can be divided up into four regimes. The response begins as linear for displacements of up to about 0.5 mm, followed by a plateau through which the foam continues to displace despite minimal increase in load. At around 0.95 mm, the loads start to increase again, producing a bump in the graph that continues until around 1.3 mm, when the loads begin to rise much more sharply. The linear, plateau, and sharply increasing regions all resemble behaviors expected from ideal foams [9], so the region between 0.95-1.3 mm is expected to be influenced primarily by the geometry of the corrugations.

MODELING APPROACH

A series of finite element simulations to determine the mechanical properties of the foam were conducted using ANSYS. A representative 2-D cross section of the foam was modeled in plane strain, as shown in FIG 4. The cross-section contained 2.5 corrugations over a length of 18.0 mm. A symmetry boundary condition was applied at the left. The foam was assumed to be either linear elastic or perfectly plastic, with material properties that varied between simulations. Linear elastic simulations were assigned elastic moduli on the order of 100-1000 MPa, with Poisson's Ratio of 0.3. Perfectly plastic

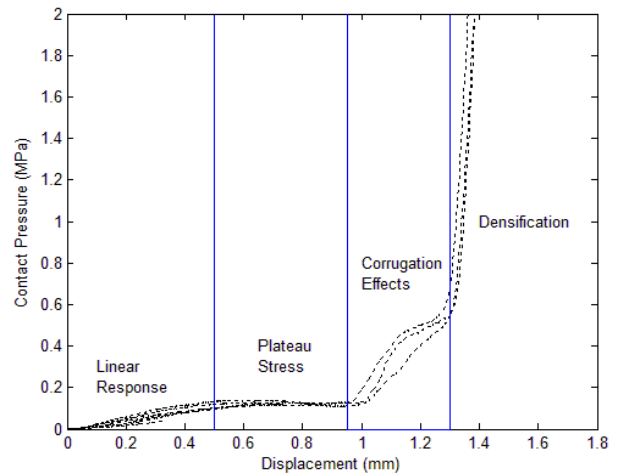


FIG 3: EXPERIMENTALLY MEASURED LOAD-VS.-DISPLACEMENT DATA

simulations were assigned the same properties as linear elastic, and additionally assigned a yield stress for which all higher strains produced the same constant stress.

The cross-sections were placed between two rigid plates, which were assigned an elastic modulus of 200 GPa. Contact pairs were assigned between the surface of the foams and the surface of the plates using ANSYS' built-in contact wizard. The contact surfaces were initially assumed to be smooth, with coefficients of friction equaling zero, but later simulations also considered coefficients of friction up to 0.2. The bottom plate was fixed in place while the top plate was moved downwards at a rate of 0.01 mm per load step for a total of 135 load steps, compressing the foam from an initial thickness of 1.50 mm down to 0.15 mm, the assumed thickness of the un-corrugated foam. At every fifth load step, the reaction forces were summed over the nodes to which displacements were applied. The reaction forces were plotted versus displacement.

RESULTS

Load versus displacement data was collected from various simulations and plotted to be compared against the data obtained experimentally. When friction is neglected, it was

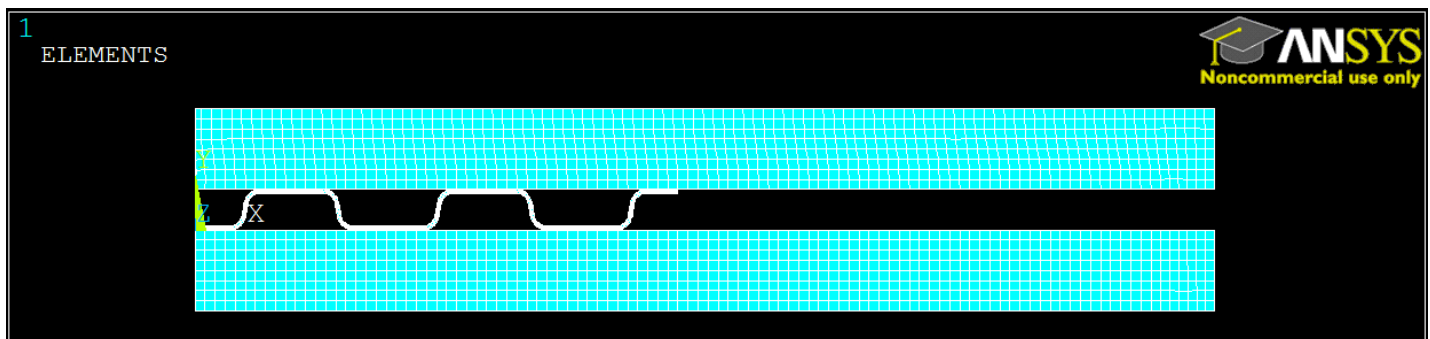


FIG 4: GEOMETRY USED TO MODEL FOAM COMPRESSION

found that an elastic modulus of about 2000 GPa, as is shown in FIG 5, best fits the initial slope of the experimentally measured data. Beginning around 0.3 mm displacement, the model data and the experimental data diverge, with the model forces increasing with displacement much more quickly than the measured forces. When yield stresses are introduced, the model forces increase at a slower rate, but still continue to diverge. The model was found to agree with experiments the longest when given a yield stress of 24 MPa for displacements of up to about 0.5 mm. Higher yield stresses produced data which continued to match the elastic forces at displacements for which the elastic data no longer agreed with experiments. Lower yield stresses produced data which diverged sooner, under-predicting the forces initially before rising sharply to exceed them.

Further simulations were performed taking the best-fit material properties obtained without friction, as shown in FIG 5, and subjecting them to different coefficients of friction, as shown in FIG 6. Though the initial slopes of the graphs increased as the coefficients of friction increased, it was seen that the overall shape of the graphs better agreed with the shape of the measured data, with forces undergoing a plateau region through the mid-range displacements before rising sharply again near the end. New elastic moduli were determined for each of the friction cases by re-fitting the initial slopes to new linear elastic materials, resulting in the data as shown in FIG 7. New yield stresses were found for each of the friction cases, resulting in the data as shown in FIG 8.

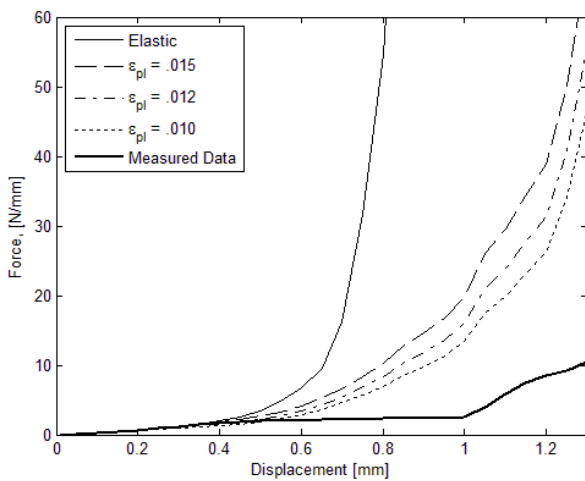


FIG 5: EFFECTS OF VARYING YIELD STRESS ON LOAD-VS-DISPLACEMENT BEHAVIOR OF A PERFECTLY PLASTIC MATERIAL WITHOUT FRICTION

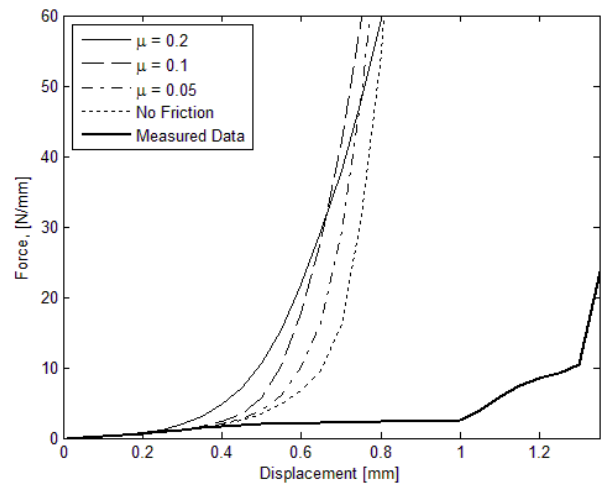


FIG 7: LOAD-VS-DISPLACEMENT BEHAVIOR OF LINEAR ELASTIC MATERIALS WITH MODULUS FITTED FOR VARIOUS FRICTION

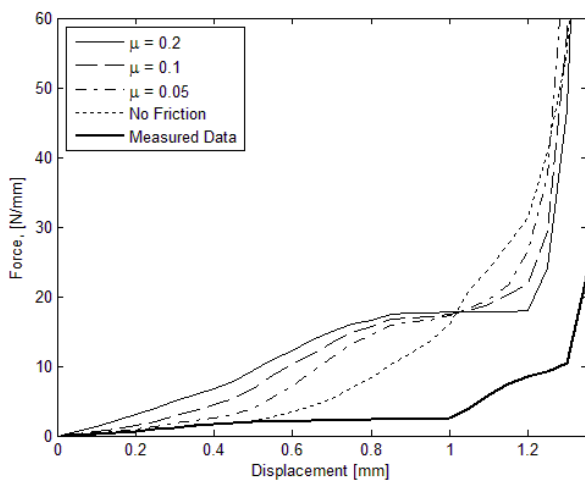


FIG 6: EFFECTS OF VARYING COEFFICIENTS OF FRICTION ON LOAD-VS-DISPLACEMENT BEHAVIOR OF A PERFECTLY PLASTIC MATERIAL

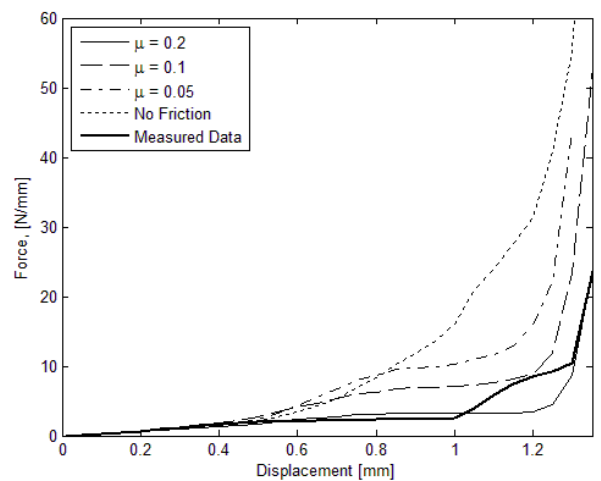


FIG 8: LOAD-VS-DISPLACEMENT BEHAVIOR OF PERFECTLY PLASTIC MATERIALS WITH MODULUS FITTED FOR VARIOUS FRICTION

CONCLUSIONS

The goal of this study was to determine the material properties needed to reproduce the load-displacement behavior from the experimental measurements in the finite element model. The plot obtained from the measured data, shown in FIG 3, displayed behavior that could be broken into four regions: an initial linear region, a plateau region, a region of increased forces which is not explained by traditional foam theory, and a final densification region in which stresses rise asymptotically.

The slope of the linear region appears to relate both to the elastic modulus of the material and to the coefficient of friction applied at the contact surface. In simulations in which the elastic modulus of the foam was increased or decreased, the entire load-displacement curve increased proportionally to the increase in modulus. In simulations in which the coefficient of friction was increased, the initial slope of the plot increased but the increase was not proportional.

The presence of the plateau region appears to rely on the presence of yielding. Whenever fully elastic materials were considered, as shown both in FIG 5 and in FIG 7, the loading curve rose sharply before any plateau could be achieved. However, the presence of yielding is not sufficient by itself to reproduce the plateau region without friction. As FIG 6 and FIG 8 show, increases in coefficients of friction result in prolonging of the plateau region, until at a coefficient of 0.2 it is able to extend through the entire plateau region and into the third region.

The models were unable to reproduce the third region. It was believed beforehand that the region might be somehow related to the corrugated geometry of the foam component, but this does not appear to be the case. Further study may be warranted in order to reproduce this region, although it is worth remembering that by the time this and other components in the SOFC stack reach such high displacements, it seems likely that other components in the stack may already have failed.

The fourth, asymptotic region occurred as the height of the compressed foam neared the same height as the thickness of uncompressed foam. At this point, the corrugations are no longer able to deflect any further, and load becomes distributed across the entire foam. It makes sense that at this point the foam takes much more force to displace, because at this point the load is being shared by the entire foam.

Further work is still needed in evaluating the mechanical performance of the FlexCell. Within the foam itself, further study is needed in order to reproduce the unexplained third region which the models so far have been unable to capture. There is also the second, anode-side foam for which a similar process must be repeated. Characterization of both foams must be repeated at higher temperatures, the results of which can be incorporated into a model which includes the rest of the SOFC stack. The stack model can then be used to assess the distribution of loads that is transferred from the foams to the PEN, in order to assess the risk of failure to the electrolyte.

ACKNOWLEDGMENTS

This project was funded in part by the Ohio Department of Development's Third Frontier Fuel Cell Program.

REFERENCES

- [1] S. M. Haile, "Fuel cell materials and components," *Acta Materialia*, vol. 51, no. 19, pp. 5981-6000, Nov. 2003.
- [2] N. Q. Minh, "Solid oxide fuel cell technology--features and applications," *Solid State Ionics*, vol. 174, no. 1, pp. 271-277, Oct. 2004.
- [3] N. Sammes, A. Smirnova, and O. Vasylyev, Eds., "Fuel Cell Technologies: State and Perspectives," vol. 202, 2005.
- [4] R. M. Ormerod, "Solid oxide fuel cells," *Chemical Society Reviews*, vol. 32, no. 1, pp. 17-28, 2003.
- [5] "NexTech unveils largest SOFC tech platform," *Fuel Cells Bulletin*, vol. 2009, no. 8, p. 1, Aug. 2009.
- [6] R. Berke, A. Suresh, and M. E. Walter, "Mechanical Characterization and Modeling of Electrolyte Membranes in Electrolyte-Supported SOFCs," in *Proceedings of the SEM 2010 Annual Conference*, 2010.
- [7] C. Lin, T. Chen, Y. Chyou, and L. Chiang, "Thermal stress analysis of a planar SOFC stack," *Journal of Power Sources*, vol. 164, no. 1, pp. 238-251, Jan. 2007.
- [8] V. Paserin, S. Marcuson, J. Shu, and D. S. Wilkinson, "The chemical vapor deposition technique for Inco nickel foam production--manufacturing benefits and potential applications," in *Cellular Metals and Metal Foaming Technology*, 2003.
- [9] M. Ashby, "The properties of foams and lattices," *Philosophical Transactions of the Royal Society A: Mathematical, Physical and Engineering Sciences*, vol. 364, no. 1838, pp. 15-30, Jan. 2006.